Chemical Science

ROYAL SOCIETY OF CHEMISTRY

EDGE ARTICLE

View Article Online
View Journal | View Issue

Cite this: *Chem. Sci.*, 2025, **16**, 23330

All publication charges for this article have been paid for by the Royal Society of Chemistry

Received 12th August 2025
Accepted 28th October 2025

DOI: 10.1039/d5sc06143a

rsc.li/chemical-science

Cation-switchable transposition and hydrogenation of alkenes *via* interconnected reaction mechanisms

Jonathan R. E. Cobb, Henry M. Dodge, Zoe E. Stuart, Elvis D. Perez Galarza, Shrabanti Bhattacharya, Changho Yoo, Chun-Hsing Chen and Alexander J. M. Miller *

Cation-switchable catalysis is a promising strategy for modulating reaction rates or selectivity using external stimuli, with potential applications including polymer synthesis and tandem catalysis. This study establishes a deeper understanding of the mechanistic origins of cation rate promotion in systems where a hemilabile crown ether affixed to the catalyst serves as a cation receptor site, which in turn enables reactivity extensions of this platform to introduce cation-switchable alkene hydrogenation. The mechanistic study hinges on the synthesis of two previously unreported iridium(III) complexes, bearing either bis(2-methoxyethyl)amine or diethylamine groups, which could be compared in catalysis with and without cation promoters. Only the catalyst containing a crown ether exhibits switchable catalysis, providing support for a "substrate gating" mechanism in which cations tune the hemilability of the crown ether donors to enable alkene binding. The generality of the substrate gating mechanism is established through the extension of catalytic reactivity to cation-switchable alkene hydrogenation. The crown-ether-containing catalyst was found to be an effective hydrogenation catalyst capable of reducing internal and trisubstituted olefins. The isomerization and hydrogenation reactions occur at similar rates in some cases, and kinetic and labeling studies provide insight into the implications of competitive reactivity.

Introduction

Nature's enzymes are often regulated by cofactors that influence the activity or selectivity of the reaction in a phenomenon known as allostery.[1,2] For example, isocitrate dehydrogenase mediates the decarboxylation of isocitrate into α-ketoglutarate during the Krebs cycle only in the presence of dications such as Ca^{2+}, Co^{2+}, or Mg^{2+}.[3] Such allostery is a central tenet of biocatalysis, wherein enzyme–guest interactions at a distal site induce a conformational change that promotes catalysis.[4] Chemists have long sought analogously responsive synthetic catalysts, using chemical, electrochemical, or photochemical promoters/switches.[5–11] Switchable catalysts have led to breakthroughs in polymer synthesis, where unprecedented control over (multi)block copolymers is made possible, with additional applications in small molecule transformations related to tandem or cascade reactions.[8]

Among the chemical switches studied to date, cations are attractive because the wide variety of available salts can result in carefully tailored reactivity.[12] Our group has developed pincer-crown ether catalysts that pair a multidentate ligand framework with a macrocyclic cation receptor site.[13] The first version of this catalyst, $[(^{15c5}NCOP^{iPr})IrH][BAr^F{}_4]$ (Ar^F = 3,5-bis(trifluoromethyl)phenyl), contained an aza-15-crown-5 ether receptor that enabled alkene isomerization with switchable and tunable activity using Li^+ as the "on switch" and Cl^- as the "off switch" (Fig. 1A).[14] The turnover frequency (TOF) for allylbenzene positional isomerization with $[(^{15c5}NCOP^{iPr})IrH]^+$ alone was low, but together with $LiBAr^F{}_4 \cdot 3Et_2O$ the catalytic activity increased by more than a factor of 1000 to reach a TOF of 2000 h^{-1}.[14] A catalyst with a larger, Na^+-selective aza-18-crown-6 ether moiety was capable of alkene transposition over multiple sites, enabling cation-switchable selectivity where the 2-(*E*)-isomer was formed without Na^+ and the 3-isomer was formed when Na^+ was present.[15] These catalysts are among the fastest known for transpositional alkene isomerization.

We have considered two possibilities for the mechanism of cation-induced reaction rate promotion in catalysis. The cations could be modulating the hemilability of the crown ether, gating substrates from accessing the active site (Fig. 1B). When no cations are present, alkenes are prevented from binding the iridium center because the active site is blocked by crown ether donors. When cations are present, alkene binding becomes favorable due to the formation of cation–crown interactions which provide an open coordination site for the alkene. An additional possibility is that the positively charged ion in the crown ether could induce a local electric field, lowering

Department of Chemistry, University of North Carolina at Chapel Hill, Chapel Hill, NC, USA. E-mail: ajmm@email.unc.edu

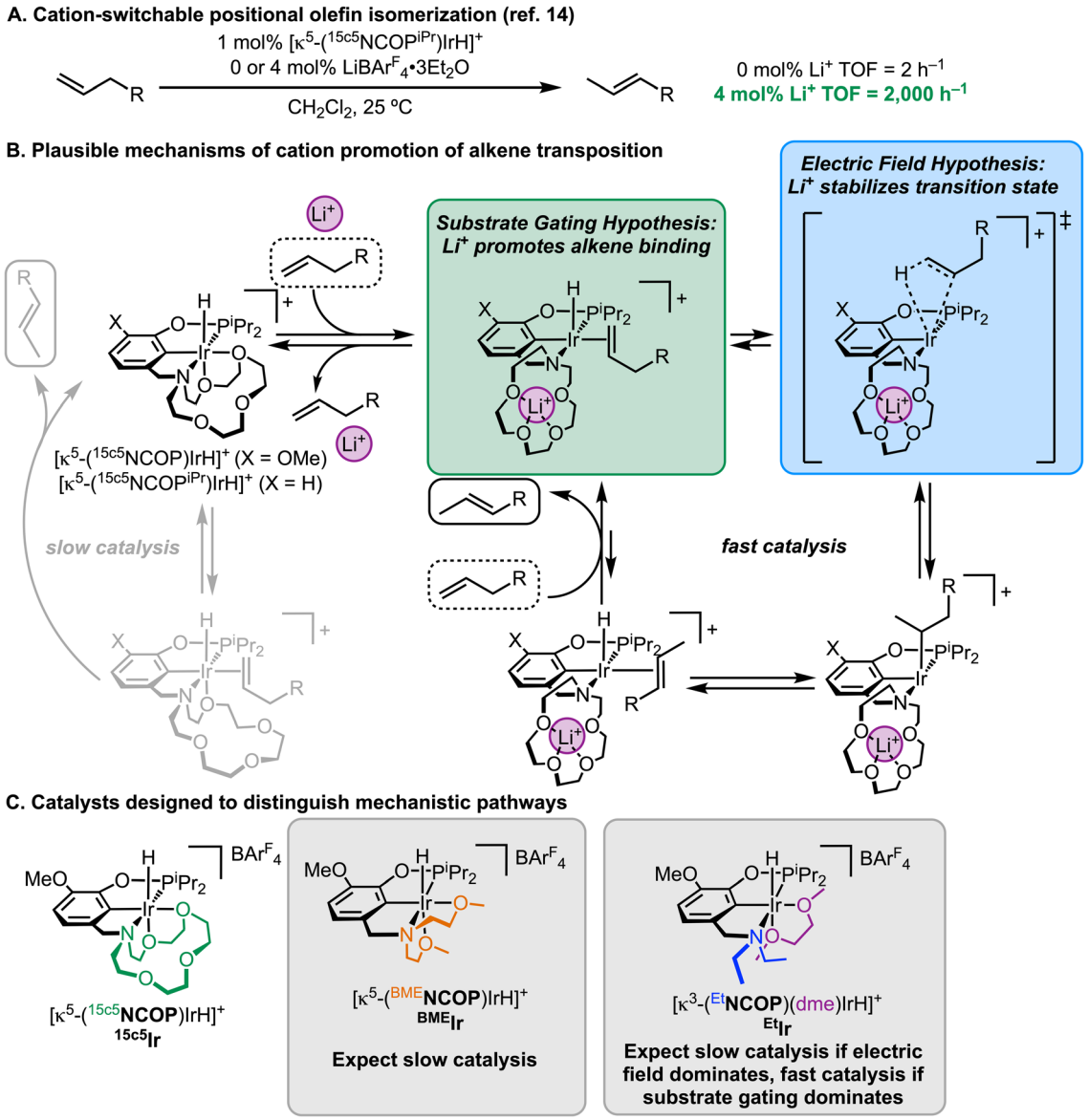

Fig. 1 (A) Cation-switchable positional isomerization of alkenes. (B) Mechanistic proposal highlighting two hypotheses for the origin of cation promotion: substrate gating (cation-tuned hemilability) and electric field effects. (C) Three catalysts designed to probe cation-responsive catalysis mechanisms.

turnover-limiting activation energy (Fig. 1B).[16,17] We were eager to understand which of these mechanisms was the dominant factor in controlling catalysis, which could have broader implications in the design of cation-switchable catalysts.

Fig. 1C shows the three catalysts that were designed to systematically disentangle substrate gating (cation-tunable hemilability) from cation-induced electric field effects. The catalyst ^{15c5}**Ir** features the original pincer-crown ether ligand, which can engage in hemilabile ether binding to Ir and can support strong cation–macrocycle interactions. The catalyst ^{BME}**Ir** bears a bis(2-methoxyethyl)amine group, which can still support hemilabile ether binding to Ir but would be expected to have a low binding affinity for cations. Finally, the complex ^{Et}**Ir** features only a diethylamine group and is unable to engage in significant donation either to Ir or to cations.

If substrate gating is the primary mechanism of cation promotion, and electric fields imparted by the proximal cation are negligible, the rate of isomerization by ^{Et}**Ir** should be similar to ^{15c5}**Ir** with the lithium activator. Conversely, if the local electric fields of the proximal cation are essential to the rapid rates of isomerization, then ^{Et}**Ir**—which cannot localize a positive charge near the metal center—should be much slower than the original system. ^{BME}**Ir** should react slowly both with and without Li^+ due to its lack of a cation receptor site, serving as an important control.

The two plausible mechanisms would also be expected to have different behavior when expanded beyond the original context of alkene transposition. Electric field effects are expected to be fairly narrow in reaction scope, based on the exact nature of the transition state structure and how it might be

influenced by a local positive charge.[18] A substrate gating mechanism, conversely, should be much more general: analogous cation promotion would be expected for many other reactions that rely on an olefin binding step (alkene hydrogenation, in this case).

The results of a comparative study of iridium pincer catalysts for alkene transposition and hydrogenation are reported here. Only the pincer-crown ether catalyst, with a macrocyclic cation receptor group, is capable of switchable catalysis. The maximum rate of the pincer-crown ether catalyst is very similar to a model catalyst without a macrocycle, consistent with a substrate gating mechanism—rather than electric field effects—explaining the cation rate-promotion effects. A rare example of switchable alkene hydrogenation catalysis is also reported, demonstrating the generality of substrate gating to control additional alkene reactions. The isomerization and hydrogenation reactions are found to be mechanistically linked, with positional isomerization and hydrogenation occurring on the same time scale in substrates capable of isomerization. The mechanistic probes introduced here provide insight into the mechanism of a high-performing class of switchable catalyst, while also offering a more broadly applicable approach to understanding and advancing cation-switchable catalysis.

Results and discussion

Synthesis of iridium complexes

The macrocycle-containing pincer-crown ether catalyst **^{15c5}Ir**, with a methoxy group included in the backbone to improve catalyst resistance to arene cyclometallation, was prepared as previously reported.[19] To access **^{BME}Ir**, the previously reported hydrido chloride complex κ^4-(^{BME}NCOP)IrH(Cl)[20] was treated with NaBAr$^F_4$ to abstract the chloride ligand and induce ether chelation. The cationic hydride complex **^{BME}Ir** was obtained in 96% yield (Fig. 2). Characterization details are provided in the following section.

A similar synthetic strategy was attempted to access **^{Et}Ir** *via* chloride abstraction from the previously reported dimer [κ^4-(^{Et}NCOP)IrH(Cl)]$_2$.[20] However, independent reactions of the chloride-bridged dimer with NaBAr$^F_4$, AgBAr$^F_4$, LiBAr$^F_4$, [Li][Al(OC(CF$_3$)$_3$)$_4$], and [Ph$_3$C][BAr$^F_4$] in PhCl or CH_2Cl_2 revealed little or no conversion to the target cationic product. At first, we turned to treatment with TlBAr$^F_4$ in CH_2Cl_2 in the presence of 5 equiv. 1,2-dimethoxyethane (dme), which resulted in formation of a white precipitate presumed to be TlCl. As shown in Fig. 3, the reaction proceeded in 93% yield to the dme adduct of

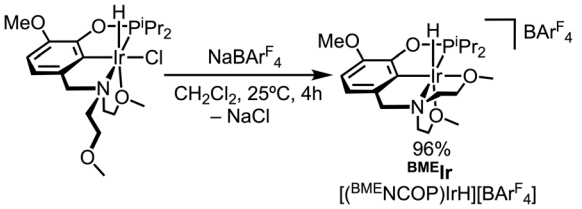

Fig. 2 Synthesis of [(^{BME}NCOP)IrH][BAr$^F_4$] (^{BME}Ir).

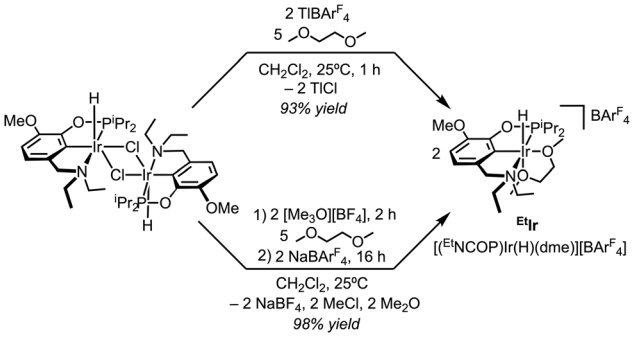

Fig. 3 Synthetic routes to [(^{Et}NCOP)Ir(H)(dme)][BAr$^F_4$] (^{Et}Ir).

cationic hydride **^{Et}Ir**. After developing this procedure, we became aware that trimethyloxonium (Me_3O^+) could be utilized for halide abstraction in some cases,[21] so we examined this reagent as a potential alternative with fewer toxicity concerns. Treating the dimer with 2 equiv. [Me$_3$O][BF$_4$] in CH_2Cl_2 in the presence of excess dme followed by anion exchange with 2 equiv. NaBAr$^F_4$ provided **^{Et}Ir** in 98% yield and established a second route to the desired catalyst. Characterization details are provided in the following section.

Comparing catalyst structural and spectroscopic properties

^{1}H NMR spectroscopy and single-crystal X-ray diffraction (XRD) analyses of the three complexes suggest weaker donation from dme compared to the ethers tethered to the pincer framework (Fig. 4). The hydride resonances of **^{15c5}Ir** (^{1}H $\delta = -29.9$ ppm) and **^{BME}Ir** (^{1}H $\delta = -30.1$ ppm) had almost identical chemical shifts, consistent with a similar degree of donation from the ether *trans* to the hydride. The hydride resonance of complex **^{Et}Ir** (^{1}H $\delta = -31.0$), however, was found approx. 1 ppm upfield of the signals for **^{15c5}Ir** and **^{BME}Ir**, which is consistent with weaker donation from the dme ligand in **^{Et}Ir** compared to the pendent ethers in **^{15c5}Ir** and **^{BME}Ir**. Trends in the length of the Ir–O bond *trans* to the hydride (Ir–O4) mirror trends seen in the NMR spectroscopic analysis, with **^{15c5}Ir** and **^{BME}Ir** having very similar Ir–O4 distances, while **^{Et}Ir** has a *ca.* 0.1 Å longer Ir–O4 distance. The shorter Ir–O4 distances are likely related to the ether donors being part of larger chelates, as reflected in longer Ir–N distances and more acute N–Ir–O4 angles in **^{15c5}Ir** and **^{BME}Ir** relative to **^{Et}Ir** (Fig. 4 and Table 1).

Cation-modulated transpositional alkene isomerization

The three cationic iridium hydride complexes were tested as catalysts for positional alkene isomerization with and without Li^+ salts. The substrate 1-triisopropylsiloxybut-3-ene (1-TIPSO-but-3-ene) was selected for the comparative study because its five possible alkene isomers enable studies of both activity and regio- and stereoselectivity differences, and because it does not contain an arene group, which can bind Ir in some cases (see Fig. 5 for naming convention).[19] The doubly transposed (*E*)-1-ene product is the thermodynamically favored isomer.[15] The three catalysts were tested under conditions of 2 mol% catalyst, 0.5 M substrate, with or without 2.2 mol% LiBAr$^F_4$·3Et$_2$O, at

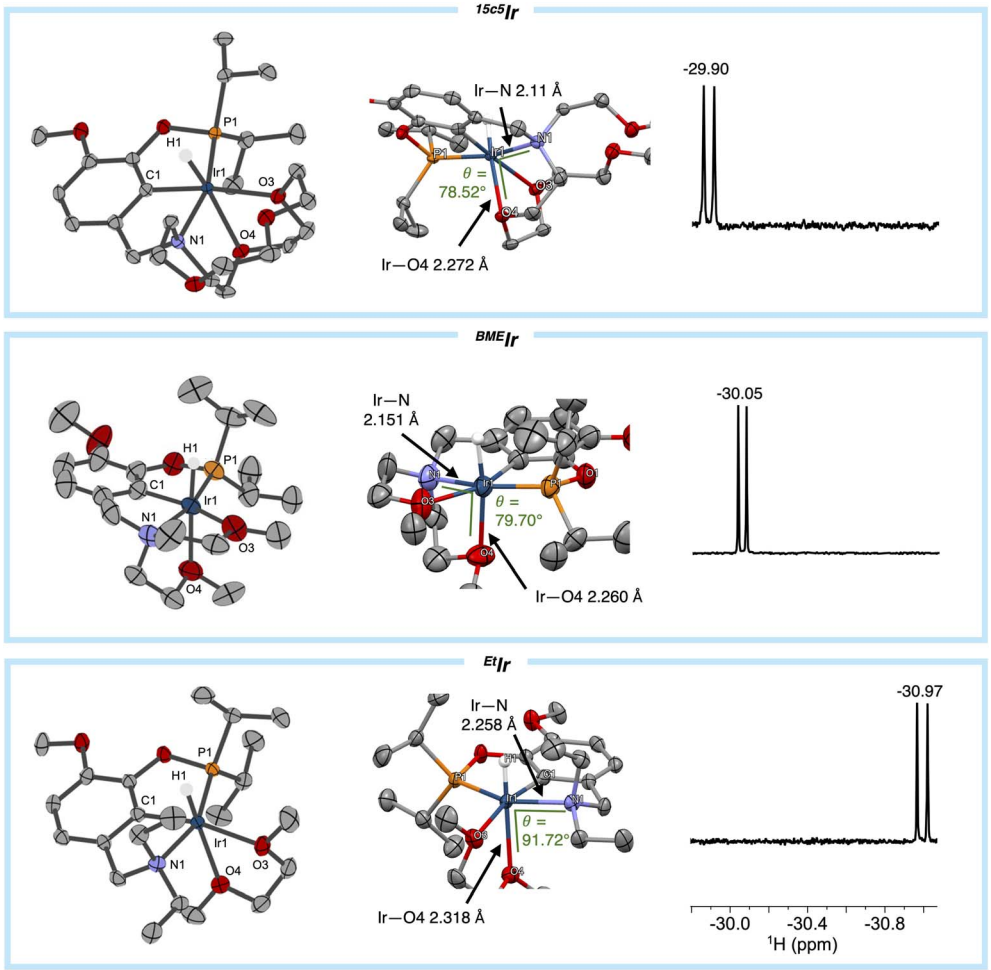

Fig. 4 Structural and spectroscopic comparisons across the three iridium catalysts. Molecular structures with ellipsoids drawn at the 50% probability level are shown at left, with hydrogen atoms (except for the hydride), solvent molecules, and counterions omitted for clarity. Structure for ^{15c5}Ir reproduced from the literature.[21] Alternative views highlighting key metrical parameters are shown in the center. ^{1}H NMR spectra of the hydride region are shown at right.

Table 1 Selected bond angles (°) and distances (Å) for the X-ray diffraction structures

Bond/angle	^{15c5}Ir	^{BME}Ir	^{Et}Ir
Ir–P	2.210(1)	2.202(2)	2.213(9)
Ir–N	2.11(3)	2.151(7)	2.258(3)
Ir–O3	2.326(3)	2.250(6)	2.263(2)
Ir–O4	2.272(3)	2.260(6)	2.318(3)
N–Ir–O3	91.73(12)	76.7(3)	92.76(10)
N–Ir–O4	78.52(12)	79.7(2)	91.72(10)

room temperature. The reactions were monitored by ^{1}H NMR spectroscopy, and kinetics were assessed by comparing first-order half-lives of the starting olefin and any olefin intermediates, acquired from the k_{obs} values of these reactions (see SI for complete kinetic analysis information).

The macrocycle-containing catalyst ^{15c5}Ir exhibited the expected switchable catalysis behavior. In the presence of Li^{+}, ^{15c5}Ir is highly active, converting the terminal alkene to the 2-ene with a half-life of 4.5 min and forming the 1-ene with a half-life of 520 min (Fig. 5). In the absence of Li^{+}, the reaction proceeds lethargically, with a half-life of over 100 000 min to produce the 2-ene. Only traces of the 1-ene (<1% of total product) were observed after 5 h. The reactivity ratio, the initial TOF with Li^{+} divided by the TOF without Li^{+}, was 130 for the first isomerization (Fig. 5B). This reactivity is similar to prior reports of isomerization with this catalyst;[14] however, the non-macrocyclic catalysts ^{BME}Ir and ^{Et}Ir had not previously been tested for cation-promoted alkene isomerization.

The bis(methoxyethyl)-based catalyst ^{BME}Ir is a slow catalyst that responds weakly to lithium salts. With no cations present, ^{BME}Ir performs the first isomerization with a 4100 min half-life, and only traces of the doubly isomerized product were observed after several days. With cations present, the rates of the first isomerization by ^{BME}Ir were *ca.* 2.5 times faster than without Li^{+}, much less than the 130-fold Li^{+} rate acceleration for ^{15c5}Ir. We hypothesize that the acyclic ethers are hemilabile to a similar degree as the crown ether, explaining the similar rate in the absence of cationic stimuli. However, though ^{BME}Ir has

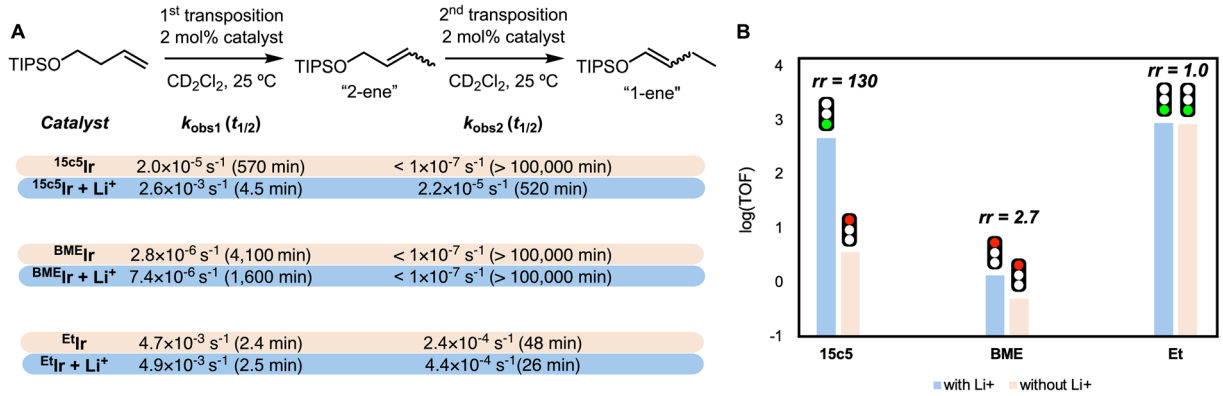

Fig. 5 (A) Summary of k_{obs} and $t_{1/2}$ values for 1-triisopropylsilyloxy-but-3-ene isomerization by the three iridium catalysts. (B) Log(TOF) plot for first isomerization by catalyst with reactivity ratio values (rr = TOF in active state/TOF in inactive state) capping each bar. Both ^{Et}**Ir** TOF values are plotted as the lower bound (SI Section III).

two donors available to coordinate with Li^+, the catalyst does not have a macrocyclic receptor site for cations, and so the interactions are insufficient to meaningfully modulate the substrate binding equilibrium.[22] This comparison highlights the necessity of polyethers for establishing strong oxygen–Li^+ interactions that enable switchable reactivity.[22–24]

^{Et}**Ir**, with a simple diethylamine moiety and a separate dme chelate, exhibits high activity both in the absence and presence of cations. The first transposition proceeds with a half-life of less than 3 min with and without Li^+. Kinetic analysis of the second transposition revealed an approximately twofold increase in activity when Li^+ was present. This is attributed to Li^+ aiding the dissociation of dme from iridium through formation of a dme adduct of Li^+. The observed twofold rate increase when Li^+ was present with ^{Et}**Ir** is quite modest when compared to the differences seen for the macrocycle-containing catalyst ^{15c5}**Ir**. Although ^{15c5}**Ir**/Li^+ and ^{Et}**Ir** are both fast catalysts, they feature distinct stereoselectivity. The stereoselectivity of the first transposition to generate the 2-ene was more than twice as high for ^{15c5}**Ir** (20 : 1 *E* : *Z*) than for ^{Et}**Ir** (9 : 1 *E* : *Z*) (Fig. 5). It is rare for a catalyst to be both highly active and highly regio- and stereoselective.[14,15,25] Critically, ^{Et}**Ir** supports rapid catalysis even in the absence of salts, as the substrate is not effectively prevented from binding, which precludes switchable catalysis.

If electric field effects were responsible for modulating activity in the presence of cations, then slow rates from both ^{BME}**Ir** and ^{Et}**Ir** would be expected as neither can retain Li^+ near Ir. Alternatively, if substrate gating was the governing factor, then ^{Et}**Ir** would be expected to operate quickly with or without Li^+, reflective of the dme ligand's high lability. Similarly, ^{BME}**Ir** would be expected to operate slowly in all cases due to a higher Ir–O dissociation equilibrium constant in a pincer framework ether compared to dme. A comparison of the isomerization rates reveals that ^{Et}**Ir** with or without Li^+ operates in a similar range to catalyst ^{15c5}**Ir**/Li^+. ^{Et}**Ir** was found to be slightly faster than the pincer-crown-ether-containing catalyst ^{15c5}**Ir**, which we attribute to the slightly larger steric profile of the crown ether relative to two ethyl groups. This comparative study of positional isomerization catalysis therefore strongly supports the substrate gating mechanism.

Prior thermodynamic and spectroscopic studies provided compelling evidence for selective binding of Li^+ to the macrocyclic portion of the catalyst. The alkali metal cation binding affinity to Ni and Ir model complexes was studied previously, with 1 : 1 Li^+ binding to 15-crown-5 moieties found to be 29 times stronger than Na^+ binding.[26] Mass spectrometry and crystallography provide additional evidence for cation binding to the crown ether when the NCOP ligand is coordinated to the transition metal in a tridentate fashion.[26] Mirroring the binding affinity studies, Li^+ activates the Ir catalyst for allylbenzene isomerization to reach rates *ca.* 1000 times faster than Na^+ or K^+ salts.[14] Kinetic analysis provided a rate law that shifts as a function of Li^+ concentration, consistent with a change in resting state from the ^{15c5}**Ir** to the Li^+ adduct of this species (structurally characterized for arene-containing substrates).[19] These studies showed that Li^+ bound to the crown ether in ^{15c5}**Ir**, but could not distinguish between tunable hemilability and electric field effects being responsible for the rate increases. We now have spectroscopic, thermodynamic, and kinetic data supporting the substrate-gating mechanism.

Cation-switchable alkene hydrogenation

We expected that if the mechanism of cation control on reactivity is substrate gating, then other reactions that rely on olefin binding at Ir should also have similar switchable catalytic behavior. On the other hand, a local electric field stabilizing a transition state might not be general, since each reaction is likely to have a distinct turnover-limiting step. Accordingly, we initiated a study of cation-switchable alkene hydrogenation with the subject iridium catalysts.

The time course plot of Fig. 6A shows that cation-switchable hydrogenation is possible using Li^+ to activate the catalyst and the organic macrocycle 12-crown-4 to sequester the cation and deactivate the catalyst. When *o*-(trifluoromethyl)styrene was allowed to react with 2 mol% ^{15c5}**Ir** for 21 h under 1 atm H_2, just 1.2% of the corresponding ethylbenzene product was observed *via* ^{1}H NMR spectroscopy. However, the addition of 2 equiv.

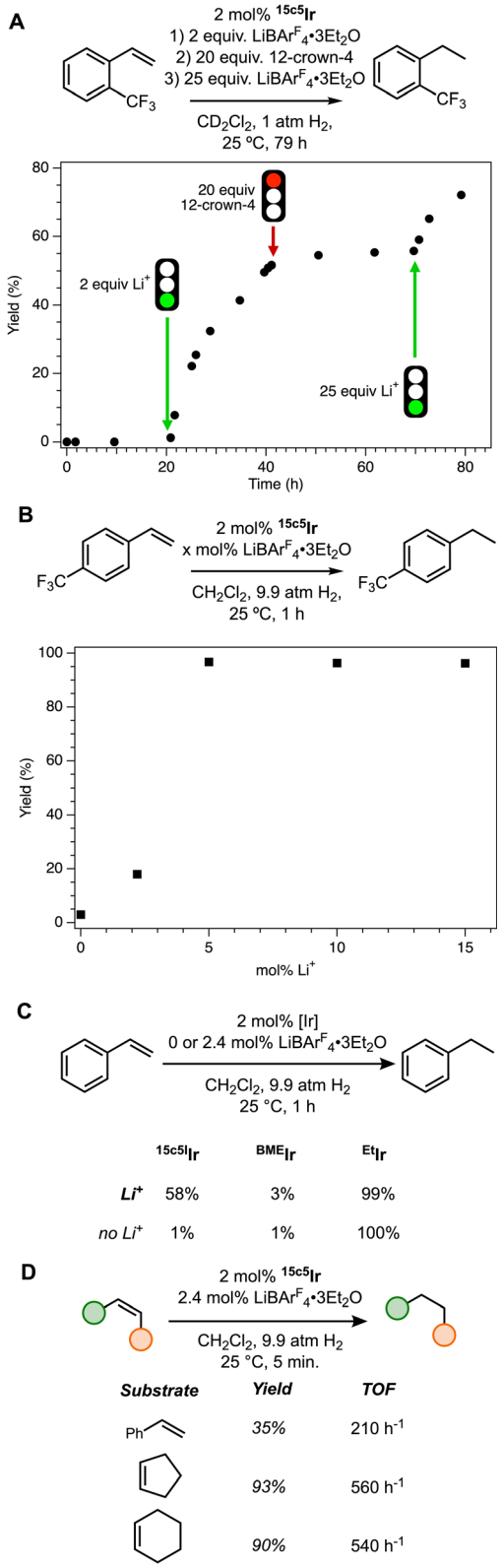

Fig. 6 (A) Cation-controlled hydrogenation of *o*-(trifluoromethyl)styrene with ^{15c5}**Ir**. Conditions listed in previous paragraph in dichloromethane solvent. The arrows denote the times at which various reagents, with equivalents listed relative to ^{15c5}**Ir**, were added. (B) Plot showing hydrogenation rate acceleration of *p*-(trifluoromethyl)styrene with increasing Li^+ loading. (C) Styrene hydrogenation yields with each catalyst in the presence or absence of Li^+. (D) Yield and TOF values from short 5-minute alkene hydrogenations.

$LiBAr^F_4 \cdot 3Et_2O$ to the mixture initiated the reaction, affording 50% *o*-(trifluoromethyl)ethylbenzene in 20 h. The addition of 20 equiv. 12-crown-4 (maintaining the H_2 atmosphere) effectively stopped the reaction, while adding additional $LiBAr^F_4 \cdot 3Et_2O$ re-initiated reaction progress to finally afford 72% of the alkane product in 79 h total. This experiment offered promising evidence that we could generalize previously reported switchable catalysis to the realm of hydrogenation.

To maximize catalytic activity, sufficient amounts of Li^+ must be present. Comparing the yield of hydrogenation of *p*-(trifluoromethyl)styrene in the presence of 5, 10, and 15 mol% $LiBAr^F_4 \cdot 3Et_2O$, a rapid saturation in activity was observed (Fig. 6B). This aligns with prior studies of isomerization suggesting that Li^+ binding to the crown ether in the catalyst is sufficiently strong under these conditions that no further rate enhancement is observed after the first few equivalents.[14,19,26,27]

The hydrogenation reactions were sufficiently rapid that NMR-scale reactions suffered from mass transport limitations associated with the dissolution of H_2 gas, causing unreliable kinetics. Therefore, we utilized high-pressure reactors in subsequent studies to ensure ample H_2 was present in solution throughout the reaction. Under these conditions, we compared the styrene hydrogenation reactivity of ^{15c5}**Ir**, ^{BME}**Ir**, and ^{Et}**Ir** (Fig. 6C). The same reactivity trends observed for isomerization are observed for hydrogenation, with ^{BME}**Ir** giving only 1% ethylbenzene in the absence of Li^+ and 3% with added Li^+, reflective of the slight rate enhancement by Li^+ in the positional alkene isomerization study. ^{Et}**Ir** provided 100% yield without Li^+ and 99% with Li^+; ^{BME}**Ir** is always inactive and ^{Et}**Ir** is always active. Only ^{15c5}**Ir** can switch between off and on states using Li^+ as a regulatory cofactor, giving 58% yield in the active state and only 1% yield with no Li^+ present. This provides further support for the substrate gating hypothesis, and suggests the mechanism can be applied across reaction classes.

There are not many examples of switchable catalytic alkene hydrogenation. Choudhury and co-workers disclosed the use of *N*-heterocyclic carbene ligand frameworks to accomplish acid/base-controlled hydrogenation of quinoxalines at iridium.[28] Additionally, Fan and co-workers presented cation-controlled host–guest interactions to demonstrate asymmetric hydrogenation of cinnamate esters at rhodium, with activity augmented *via* the addition of cations; they later reported a pH-controlled molecular shuttle to aid in the hydrogenation of α,β-dehydroamino acid esters and aryl enamides.[29,30] Hydrogenation is a fundamental transformation in industries that rely on catalysis, for example constituting *ca.* 14% of all transformations for active pharmaceutical ingredient (API) synthesis.[31] Therefore, expanding the library of control mechanisms over this important reaction is impactful to the synthetic chemist.

It is valuable to make comparisons between cation-switchable hydrogenation and isomerization. Initial rates studies (Fig. 6D) provided TOF values for styrene hydrogenation (200 h^{-1}) and cyclic alkenes (*ca.* 550 h^{-1}) that are in the same order of magnitude as the first positional isomerization of 1-TIPSO-but-3-ene. The reactivity ratios for these hydrogenations are even larger than that observed for 1-TIPSO-but-3-ene isomerization (Fig. 5) and are excellent when compared to other

chemoswitchable catalysts.[32,33] The hydrogenation rates are similar to the rate of D_2 activation established in studies of H/D exchange in this catalyst system.[34] This comparison suggests that terminal to internal alkene positional isomerization can occur on the same timescale of hydrogenation, at least for some olefins.

To establish the relative reactivity of various alkenes for hydrogenation by **^{15c5}Ir** and understand the influence of isomerization, a broader hydrogenation survey was undertaken. Fig. 7 shows the conditions and summarizes the yields produced after a 1-hour hydrogenation. In the absence of any Li^+ salt, the yield of hydrogenation was less than 10% for almost every substrate. With added $LiBAr^F_4$, however, good yields of alkanes were observed in most cases.

The series of octene isomers provide an interesting case study. Both 1-octene (**1**) and 2-octene (**2**) were fully hydrogenated within 1 hour. When the alkene was positioned deeper in the chain as in 3-octene (**3**), however, the yield of *n*-octane was lower. The similar yields for hydrogenation of **1** and **2** is the result of rapid isomerization of **1** to **2** in the few minutes between loading the reactor and pressurization with H_2. The isomerization is sufficiently fast that the true substrate is the 2-alkene for both **1** and **2**. On the other hand, isomerization from **2** to **3** is much slower than the 60 min reaction time of the hydrogenation ($t_{1/2}$ for second transposition of TIPSO-butene = 520 min). This is fortunate, because **3** is a relatively poor substrate (presumably due to the larger ethyl substituent on the alkene). A similar trend is seen for allylbenzene (**4**) and (*E*)-β-methylstyrene (**5**), which are related by a single positional isomerization and produce *n*-propylbenzene in similar yields. Again, isomerization from the terminal alkene to the internal alkene occurs by the time H_2 is added, so the reactions are effectively the same.

Other disubstituted alkenes generally gave high yields of hydrogenation. Cyclic alkenes **21** and **22** gave near-complete

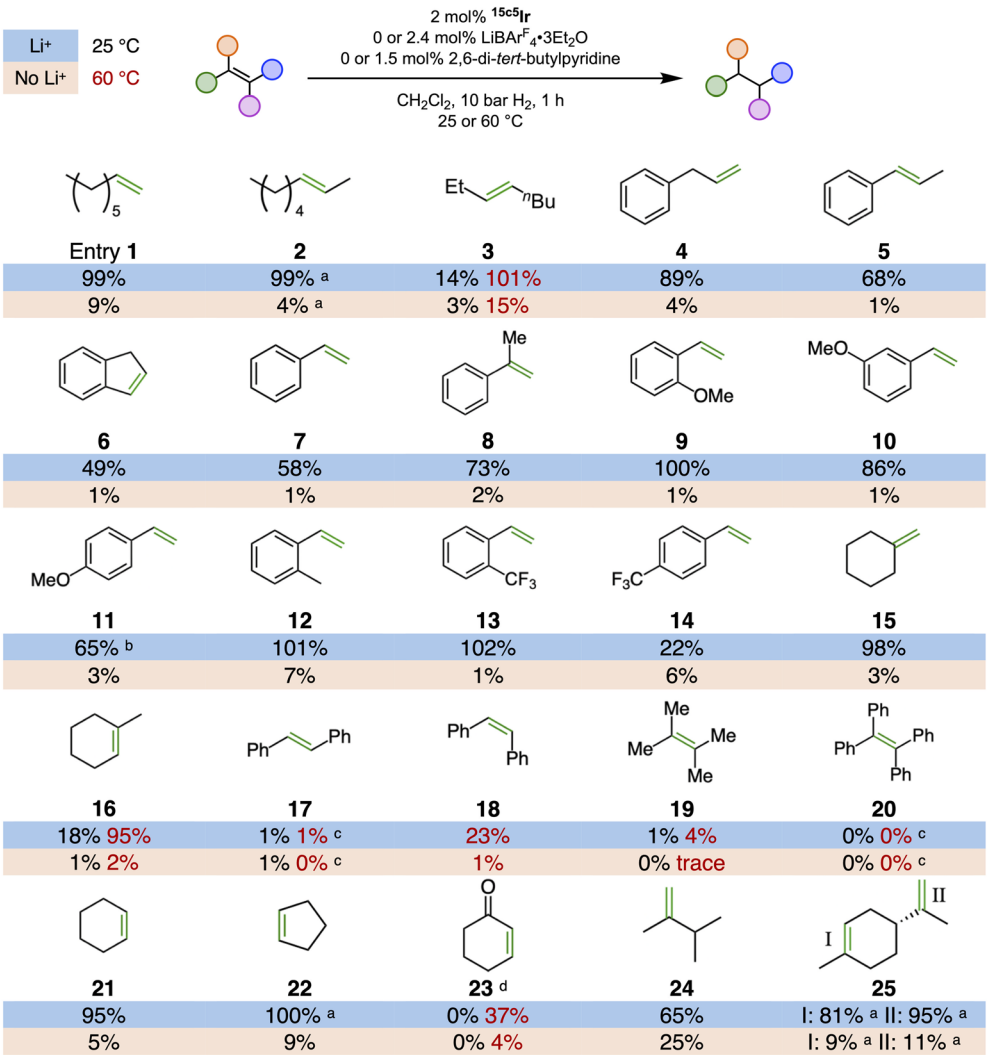

Entry	1	2	3	4	5
	99%	99% [a]	14% 101%	89%	68%
	9%	4% [a]	3% 15%	4%	1%
	6	7	8	9	10
	49%	58%	73%	100%	86%
	1%	1%	2%	1%	1%
	11	12	13	14	15
	65% [b]	101%	102%	22%	98%
	3%	7%	1%	6%	3%
	16	17	18	19	20
	18% 95%	1% 1% [c]	23%	1% 4%	0% 0% [c]
	1% 2%	1% 0% [c]	1%	0% trace	0% 0% [c]
	21	22	23 [d]	24	25
	95%	100% [a]	0% 37%	65%	I: 81% [a] II: 95% [a]
	5%	9%	0% 4%	25%	I: 9% [a] II: 11% [a]

Fig. 7 Summary of hydrogenation yields. Select substrates were chosen for reactions at 60 °C based on high steric strain and/or underperformance at 25 °C, all entries run in duplicate. Yields quantified by NMR spectroscopy, with 2% uncertainty based on the average standard deviation of each pair of runs across all substrates (details in SI). [a]Reported as the conversion of the starting alkene. [b]Traces of polystyrene were also observed. [c]Substrate not fully soluble in dichloromethane. [d]Only cyclohexanone was observed; when cyclohexanone was used as a substrate, no hydrogenation was observed (SI, Section IV).

conversion at room temperature under the standard conditions. Cyclohexenone (**23**) gave lower yields, which can be attributed to competitive carbonyl binding to the Ir inhibiting the reaction.[15] Controls with cyclohexanone confirm that no carbonyl hydrogenation was observed with ^{15c5}**Ir**/Li$^+$, establishing high chemoselectivity for alkene hydrogenation.

The 1,1-disubstituted alkene methylenecyclohexane (**15**) also was hydrogenated in high yield at room temperature. Trisubstituted 1-methyl-1-cyclohexene (**16**), which is a positional isomer of **15**, gave only 18% yield at 25 °C but showed near-complete conversion upon heating to 60 °C. Here again, the relative rates of isomerization and hydrogenation are important: if **15** was rapidly isomerized to **16**, both substrates should give low yields. Control experiments confirm that isomerization of **15** to **16** in the presence of ^{15c5}**Ir**/Li$^+$ under N_2 requires multiple days ($t_{1/2}$ *ca.* 50 h). (*Z*)- and (*E*)-stilbene were examined as a pair of substrates that could be related by *E*/*Z* isomerization (stereochemical rather than positional isomerization). In this case, (*Z*)-stilbene is preferentially hydrogenated. We hypothesize that (*E*)-stilbene is too bulky to bind well to the Ir center, precluding both hydrogenation and stereoisomerization. The result indicates that *E*/*Z* isomerization is slow in this case, which is beneficial because the less reactive *E* isomer is more thermodynamically stable—if rapid isomerization did occur, essentially no hydrogenation would be observed for (*Z*)-stilbene.

To ascertain the site of hydrogenation for alkenes that could undergo positional isomerization, a deuterium labeling study was undertaken. Under the standard reaction conditions, but with 6.8 atm D_2 instead of 9.9 atm H_2, *trans*-β-methylstyrene (**5**) was converted to isotopologues of *n*-propylbenzene with two ^{2}H NMR signals (δ = 2.56 and 1.59), corresponding to the α and β protons (Fig. 8). The ^{1}H NMR spectrum confirmed deuteration at this position, and both α and β signals integrated to 1H. Treating allylbenzene (**4**) with the same conditions revealed the same set of resonances in the ^{1}H and ^{2}H NMR spectra, consistent with D_2 addition exclusively at the internal alkene. The same trend was observed for the D_2 addition to 1-octene (**1**) and 2-octene (**2**), with exclusive internal D_2 addition. A control reaction with styrene shows that D incorporation occurs only by D_2 addition, not by other H/D scrambling pathways. Ethylbenzene formed with only 1 D atom at each of the expected positions (^{2}H NMR δ = 2.64 and 1.20).

Returning to our broader analysis of hydrogenation rates, several non-isomerizable styrene derivatives were also examined. The styrene series exhibited a significant *para*-substituent electronic effect, with the more electron-rich substrates undergoing hydrogenation more rapidly (Fig. 9A). Styrenes with *meta* and *ortho* substituents gave higher yields in each case, independent of any electronic effects. To confirm that the independent reactions accurately reflected the proclivity of the catalyst, competition experiments hydrogenating **9** and **11** in the same vial were carried out with 2 mol% ^{15c5}**Ir** or ^{Et}**Ir** and 2.4 mol% LiBAr$^F{}_4$·3Et$_2$O (Fig. 9B). After 24 hours under 1 atm H_2, a 2.2 : 1 ratio of the corresponding alkane from **9** to that of **11** was observed, confirming the higher activity of *ortho*-substituted **9**.

Initially, we speculated that the methoxy group might be binding to the Lewis acidic Li$^+$ cation in the macrocycle of the catalyst, which could enhance the hydrogenation rate. However, a competition experiment hydrogenating **9** and **11** with 2 mol%

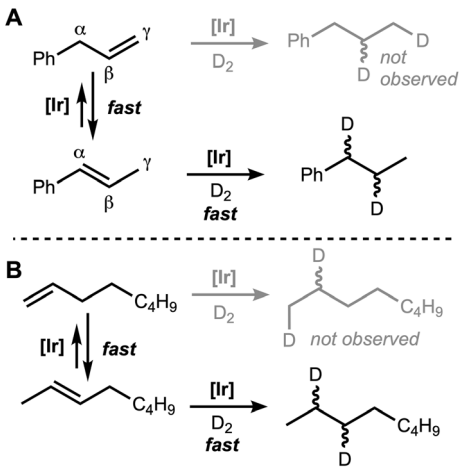

Fig. 8 Isomerization pathways to explain products observed upon D_2 addition to allylbenzene (**4**, (A)) and 1-octene (**1**, (B)) with ^{15c5}**Ir**. Conditions: 2 mol% ^{15c5}**Ir**, 2.4 mol% LiBAr$^F{}_4$·3Et$_2$OO, 6.8 atm D_2.

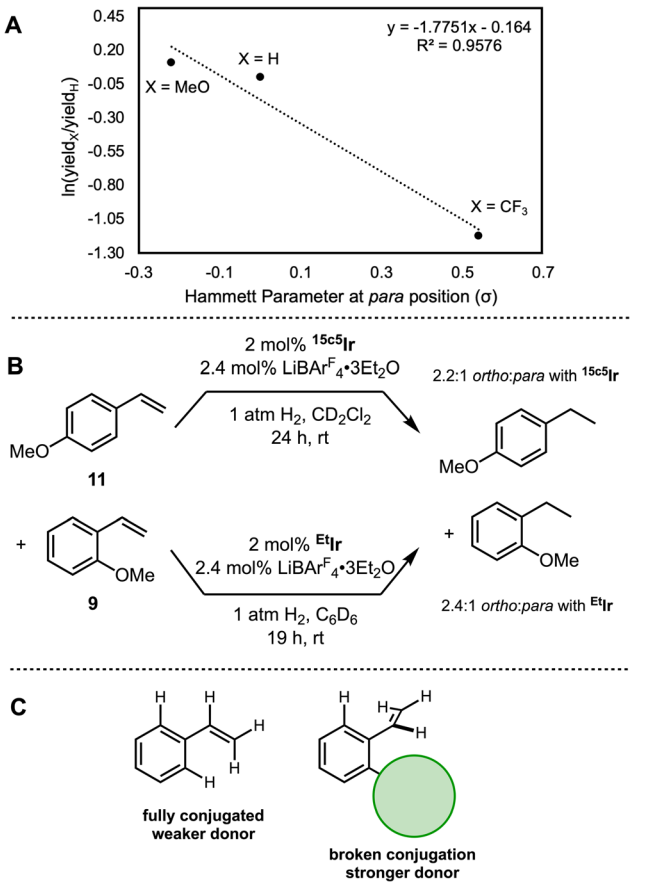

Fig. 9 (A) Hammett plot demonstrating the observed *para*-electronic effect. (B) Competition experiments of methoxy-substituted styrene derivatives with ^{15c5}**Ir** and ^{Et}**Ir**. (C) Proposed geometry of the *ortho* effect observed in catalytic hydrogenation of styrene derivatives.

^{Et}**Ir**—which has no Li^+ cation that could promote methoxy binding—still favored the product from **9** in a 2.4 : 1 ratio, ruling out the hypothesis (Fig. 9B). We also considered an iridium–methoxy interaction, but found that **12** and **13**—both of which cannot bind to Ir—both also gave 100% yield of the corresponding alkane in one hour (Fig. 7). We therefore ascribe the high reactivity to a stereoelectronic effect: any *ortho* group forces the vinyl unit out of conjugation with the aryl ring, increasing the nucleophilicity of the vinyl group, promoting binding and in turn improving activity (Fig. 9C).

The alkene/arene conjugation effect is apparent in Fig. 7 in the series moving from *ortho*-substituted styrenes (highest rates of hydrogenation), to unsubstituted styrene (**7**) which has free rotation with the conjugated rotamer preferred (and intermediate rates), to indene (**6**) which is constrained such that the alkene and arene must remain conjugated (and has the lowest rates).

Although detailed kinetic studies would be needed to establish a complete mechanism for the hydrogenation reaction, some preliminary speculation is possible by extending our prior knowledge of the mechanism of alkene transposition (Fig. 10).[15] The resting state in NMR-scale experiments was the starting complex ^{15c5}**Ir** with two ethers bound. Alkene binding promoted by Li^+ would generate a five-coordinate olefin hydride complex that is proposed to be the key intermediate in alkene isomerization (Fig. 10A). This complex has a binding site available for H_2, which would form a six-coordinate dihydrogen complex intermediate that is directly analogous to the intermediate derived from $(PCP)IrH^+$ (Fig. 10B) in a recent study of alkane transfer dehydrogenation by Goldman, Hasanayn, and co-workers.[35] Turnover could be afforded by insertion to form an alkyl, followed by alkane release either by H_2 oxidative addition and alkyl hydride reductive elimination or by direct hydrogenolysis of the alkyl in a single step (Fig. 10A, top). Another mechanistic possibility would be the microscopic reverse of the new elementary step proposed in the pathway for alkane dehydrogenation by Goldman, Hasanayn, and co-workers, which involves concerted Ir–H and C–H bond formation (Fig. 10A, bottom).[35] In the hydrogenation direction, the dihydrogen olefin hydride complex would undergo concerted hydrogen transfers from IrH and H_2 to produce the alkane σ-complex. Due to the unique geometry of this concerted

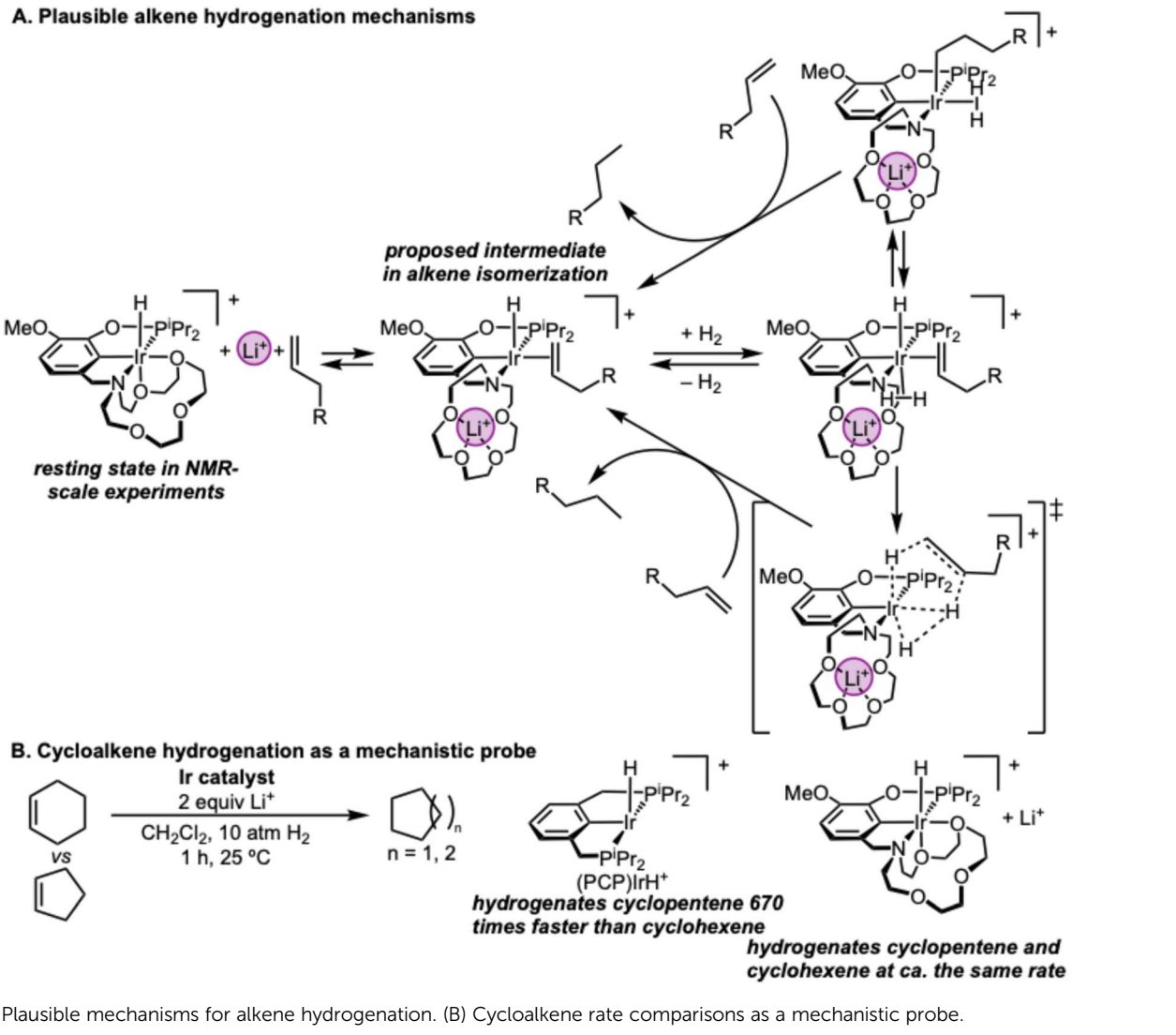

Fig. 10 (A) Plausible mechanisms for alkene hydrogenation. (B) Cycloalkene rate comparisons as a mechanistic probe.

transition state, (PCP)IrH$^+$ hydrogenates cyclopentene 670 times faster than cyclohexene. In the case of ^{15c5}**Ir**, however, a 5-minute hydrogenation of these two substrates revealed 90% yield of cyclohexane and 93% yield of cyclopentane (Fig. 6D). Therefore, the rates of hydrogenation of these two substrates with ^{15c5}**Ir** are almost the same. This would suggest a distinct mechanism of hydrogenation from (PCP)IrH$^+$, either because the bound alkene converts to alkane by the top pathway in Fig. 10A or because alkene binding to Ir is a principal contributor to the turnover-limiting step.

Conclusions

Two non-macrocyclic pincer iridium catalysts were prepared and a comparative catalysis study with the previously reported 15-crown-5-containing catalyst was undertaken. Only the macrocyclic catalyst ^{15c5}**Ir** demonstrated switchable catalytic activity, while ^{BME}**Ir** and ^{Et}**Ir** showed reaction rates minimally responsive to cations. Critically, ^{Et}**Ir** is highly active in the absence of cations, ruling out the influence of a local electric field (which the neutral amine arm of this catalyst lacks the ability to create). This reactivity supports a substrate gating mechanism reliant on the hemilability of the crown ether donors as opposed to local electric field effects stabilizing a turnover-limiting transition state. Further support for this mechanism comes from the prior observations that ^{15c5}**Ir** has high specificity for rate enhancement by Li$^+$, while the analogous catalyst with a larger aza-18-crown-6 macrocycle undergoes promotion by Na$^+$ with high specificity.[14,15]

The switchable reactivity of ^{15c5}**Ir** was extended to alkene hydrogenation, establishing the generality of the substrate gating mechanism in controlling reactions of olefins. Cyclic, mono- and 1,2-disubstituted alkenes were successfully hydrogenated in high yield at room temperature, and heating to 60 °C enabled access to more highly substituted substrates as well as long-chain alkenes. In some cases, rapid isomerization produced a new alkene that was swiftly hydrogenated at the isomerized position. In other cases, hydrogenation occurred at the original alkene position, before transposition could occur to form a more recalcitrant alkene isomer. High yields were unexpectedly obtained for *ortho*-substituted styrenes, attributed to a stereoelectronic effect in which steric interactions reduce the conjugation of the alkene. This catalyst shows promise in accessing bulky alkenes without reducing carbonyls and stands as a rare example of switchable hydrogenation catalysis.[36–39]

Author contributions

A. J. M. M. designed and supervised the project. J. R. E. C. and H. M. D. designed, conducted, and analyzed the results of synthetic, mechanistic, and catalysis experiments. Z. E. S., E. D. P., and S. B. assisted with synthesis and conducted some of the hydrogenation experiments. C.-H. C. and C. Y. collected and analyzed X-ray crystallographic data. H. M. D., J. R. E. C., and A. J. M. M. wrote the paper with input from all coauthors.

Conflicts of interest

There are no conflicts to declare.

Data availability

The data associated with this article, including NMR spectra of synthesized compounds, NMR spectra characterizing the catalytic experiments, and crystallographic data, have been included in the supplementary information (SI). Supplementary information is available. See DOI: **https://doi.org/10.1039/d5sc06143a**.

CCDC 2478806 and 2478807 contain the supplementary crystallographic data for this paper.[40a,b]

Acknowledgements

This material is based upon work supported by the National Science Foundation under Grant no. CHE-2102244 and CHE-2451966. The mass spectrometry work was supported by the NSF under grant no. CHE-1726291. The NMR spectrometry work was supported by the NSF under grant no. CHE-1828183. Matthew Porowski assisted in hydrogenation training.

References

1 A. A. S. T. Ribeiro and V. Ortiz, A Chemical Perspective on Allostery, *Chem. Rev.*, 2016, **116**(11), 6488–6502, DOI: **10.1021/acs.chemrev.5b00543**.
2 H. N. Motlagh, J. O. Wrabl, J. Li and V. J. Hilser, The Ensemble Nature of Allostery, *Nature*, 2014, **508**(7496), 331–339, DOI: **10.1038/nature13001**.
3 T. Ma, Y. Peng, W. Huang, Y. Liu and J. Ding, The β and γ Subunits Play Distinct Functional Roles in the α2βγ Heterotetramer of Human NAD-Dependent Isocitrate Dehydrogenase, *Sci. Rep.*, 2017, **7**(1), 41882, DOI: **10.1038/srep41882**.
4 R. Nussinov, Introduction to Protein Ensembles and Allostery, *Chem. Rev.*, 2016, **116**(11), 6263–6266, DOI: **10.1021/acs.chemrev.6b00283**.
5 S. Deng, B. J. Jolly, J. R. Wilkes, Y. Mu, J. A. Byers, L. H. Do, A. J. M. Miller, D. Wang, C. Liu and P. L. Diaconescu, Spatiotemporal Control for Integrated Catalysis, *Nat. Rev. Methods Primers*, 2023, **3**(1), 28, DOI: **10.1038/s43586-023-00207-0**.
6 A. M. Lifschitz, M. S. Rosen, C. M. McGuirk and C. A. Mirkin, Allosteric Supramolecular Coordination Constructs, *J. Am. Chem. Soc.*, 2015, **137**(23), 7252–7261, DOI: **10.1021/jacs.5b01054**.
7 A. J. McConnell, C. S. Wood, P. P. Neelakandan and J. R. Nitschke, Stimuli-Responsive Metal–Ligand Assemblies, *Chem. Rev.*, 2015, **115**(15), 7729–7793, DOI: **10.1021/cr500632f**.
8 T. Stößer, T. T. D. Chen, Y. Zhu and C. K. Williams, 'Switch' Catalysis: From Monomer Mixtures to Sequence-Controlled Block Copolymers, *Philos. Trans. R. Soc., A*, 2017, **376**(2110), 20170066, DOI: **10.1098/rsta.2017.0066**.

9 M. Raynal, P. Ballester, A. Vidal-Ferran and P. W. N. M. van Leeuwen, Supramolecular Catalysis. Part 1: Non-Covalent Interactions as a Tool for Building and Modifying Homogeneous Catalysts, *Chem. Soc. Rev.*, 2014, **43**(5), 1660–1733, DOI: 10.1039/C3CS60027K.

10 M. Vlatković, B. S. L. Collins and B. L. Feringa, Dynamic Responsive Systems for Catalytic Function, *Chem.–Eur. J.*, 2016, **22**(48), 17080–17111, DOI: 10.1002/chem.201602453.

11 M. Raynal, P. Ballester, A. Vidal-Ferran and P. W. N. M. van Leeuwen, Supramolecular Catalysis. Part 2: Artificial Enzyme Mimics, *Chem. Soc. Rev.*, 2014, **43**(5), 1734–1787, DOI: 10.1039/C3CS60037H.

12 C. Yoo, H. M. Dodge and A. J. M. Miller, Cation-Controlled Catalysis with Crown Ether-Containing Transition Metal Complexes, *Chem. Commun.*, 2019, **55**(35), 5047–5059, DOI: 10.1039/C9CC00803A.

13 S. Acosta-Calle and A. J. M. Miller, Tunable and Switchable Catalysis Enabled by Cation-Controlled Gating with Crown Ether Ligands, *Acc. Chem. Res.*, 2023, **56**(8), 971–981, DOI: 10.1021/acs.accounts.3c00056.

14 M. R. Kita and A. J. M. Miller, An Ion-Responsive Pincer-Crown Ether Catalyst System for Rapid and Switchable Olefin Isomerization, *Angew. Chem., Int. Ed.*, 2017, **56**(20), 5498–5502, DOI: 10.1002/anie.201701006.

15 A. M. Camp, M. R. Kita, P. T. Blackburn, H. M. Dodge, C.-H. Chen and A. J. M. Miller, Selecting Double Bond Positions with a Single Cation-Responsive Iridium Olefin Isomerization Catalyst, *J. Am. Chem. Soc.*, 2021, **143**(7), 2792–2800, DOI: 10.1021/jacs.0c11601.

16 K. Kang, J. Fuller, A. H. Reath, J. W. Ziller, A. N. Alexandrova and J. Y. Yang, Installation of Internal Electric Fields by Non-Redox Active Cations in Transition Metal Complexes, *Chem. Sci.*, 2019, **10**(43), 10135–10142, DOI: 10.1039/C9SC02870F.

17 A. Maitra, W. R. Lake, A. Mohamed, S. C. Edington, P. Das, B. C. Thompson, S. Hammes-Schiffer, M. Johnson and J. M. Dawlaty, Measuring the Electric Fields of Ions Captured in Crown Ethers, *J. Phys. Chem. Lett.*, 2024, **15**(29), 7458–7465, DOI: 10.1021/acs.jpclett.4c01303.

18 S. A. Siddiqui, T. Stuyver, S. Shaik and K. D. Dubey, Designed Local Electric Fields—Promising Tools for Enzyme Engineering, *JACS Au*, 2023, **3**(12), 3259–3269, DOI: 10.1021/jacsau.3c00536.

19 H. M. Dodge, M. R. Kita, C.-H. Chen and A. J. M. Miller, Identifying and Evading Olefin Isomerization Catalyst Deactivation Pathways Resulting from Ion-Tunable Hemilability, *ACS Catal.*, 2020, **10**(21), 13019–13030, DOI: 10.1021/acscatal.0c03784.

20 C. Yoo, H. M. Dodge, A. H. Farquhar, K. E. Gardner and A. J. M. Miller, Decarbonylative Ether Dissection by Iridium Pincer Complexes, *Chem. Sci.*, 2020, **11**(44), 12130–12138, DOI: 10.1039/D0SC03736B.

21 P. D. Vu, A. J. Boydston and C. W. Bielawski, Ionic Liquids via Efficient, Solvent-Free Anion Metathesis, *Green Chem.*, 2007, **9**(11), 1158–1159, DOI: 10.1039/B705745H.

22 T. V. Tran, L. J. Karas, J. I. Wu and L. H. Do, Elucidating Secondary Metal Cation Effects on Nickel Olefin Polymerization Catalysts, *ACS Catal.*, 2020, **10**(18), 10760–10772, DOI: 10.1021/acscatal.0c02949.

23 T. V. Tran, E. Lee, Y. H. Nguyen, H. D. Nguyen and L. H. Do, Customizing Polymers by Controlling Cation Switching Dynamics in Non-Living Polymerization, *J. Am. Chem. Soc.*, 2022, **144**(37), 17129–17139, DOI: 10.1021/jacs.2c07098.

24 T. V. Tran and L. H. Do, Tunable Modalities in Polyolefin Synthesis via Coordination Insertion Catalysis, *Eur. Polym. J.*, 2021, **142**, 110100, DOI: 10.1016/j.eurpolymj.2020.110100.

25 C. R. Larsen, G. Erdogan and D. B. Grotjahn, General Catalyst Control of the Monoisomerization of 1-Alkenes to Trans-2-Alkenes, *J. Am. Chem. Soc.*, 2014, **136**(4), 1226–1229, DOI: 10.1021/ja411438d.

26 J. B. Smith, A. M. Camp, A. H. Farquhar, S. H. Kerr, C.-H. Chen and A. J. M. Miller, Organometallic Elaboration as a Strategy for Tuning the Supramolecular Characteristics of Aza-Crown Ethers, *Organometallics*, 2019, **38**(22), 4392–4398, DOI: 10.1021/acs.organomet.9b00462.

27 J. B. Smith, S. H. Kerr, P. S. White and A. J. M. Miller, Thermodynamic Studies of Cation–Macrocycle Interactions in Nickel Pincer–Crown Ether Complexes Enable Switchable Ligation, *Organometallics*, 2017, **36**(16), 3094–3103, DOI: 10.1021/acs.organomet.7b00431.

28 B. Maji and J. Choudhury, Switchable Hydrogenation with a Betaine-Derived Bifunctional Ir–NHC Catalyst, *Chem. Commun.*, 2019, **55**(31), 4574–4577, DOI: 10.1039/C9CC00972H.

29 G.-H. Ouyang, Y.-M. He, Y. Li, J.-F. Xiang and Q.-H. Fan, Cation-Triggered Switchable Asymmetric Catalysis with Chiral Aza-CrownPhos, *Angew. Chem., Int. Ed.*, 2015, **54**(14), 4334–4337, DOI: 10.1002/anie.201411593.

30 Y.-P. Tang, Y.-E. Luo, J.-F. Xiang, Y.-M. He and Q.-H. Fan, Rhodium-Catalyzed ON-OFF Switchable Hydrogenation Using a Molecular Shuttle Based on a [2]Rotaxane with a Phosphine Ligand, *Angew. Chem., Int. Ed.*, 2022, **61**(15), e202200638, DOI: 10.1002/anie.202200638.

31 J. S. Carey, D. Laffan, C. Thomson and M. T. Williams, Analysis of the Reactions Used for the Preparation of Drug Candidate Molecules, *Org. Biomol. Chem.*, 2006, **4**(12), 2337–2347, DOI: 10.1039/B602413K.

32 S. Acosta-Calle, E. Z. Huebsch, S. S. Kolmar, M. T. Whited, C.-H. Chen and A. J. M. Miller, Regulating Access to Active Sites via Hydrogen Bonding and Cation–Dipole Interactions: A Dual Cofactor Approach to Switchable Catalysis, *J. Am. Chem. Soc.*, 2024, **146**(16), 11095–11104, DOI: 10.1021/jacs.3c10877.

33 J.-C. Wasilke, S. J. Obrey, R. T. Baker and G. C. Bazan, Concurrent Tandem Catalysis, *Chem. Rev.*, 2005, **105**(3), 1001–1020, DOI: 10.1021/cr020018n.

34 M. R. Kita and A. J. M. Miller, Cation-Modulated Reactivity of Iridium Hydride Pincer-Crown Ether Complexes, *J. Am. Chem. Soc.*, 2014, **136**(41), 14519–14529, DOI: 10.1021/ja507324s.

35 A. Parihar, T. J. Emge, F. Hasanayn and A. S. Goldman, Alkane Dehydrogenation and H/D Exchange by a Cationic Pincer-Ir(III) Hydride: Cooperative C–H Addition and β-H Elimination Modes Induce Anomalous Selectivity, *J. Am.*

Chem. Soc., 2025, **147**(12), 10279–10297, DOI: **10.1021/jacs.4c16699**.

36 L. Alig, M. Fritz and S. Schneider, First-Row Transition Metal (De)Hydrogenation Catalysis Based On Functional Pincer Ligands, *Chem. Rev.*, 2019, **119**(4), 2681–2751, DOI: **10.1021/acs.chemrev.8b00555**.

37 A. Pfaltz, J. Blankenstein, R. Hilgraf, E. Hörmann, S. McIntyre, F. Menges, M. Schönleber, S. P. Smidt, B. Wüstenberg and N. Zimmermann, Iridium-Catalyzed Enantioselective Hydrogenation of Olefins, *Adv. Synth. Catal.*, 2003, **345**(1–2), 33–43, DOI: **10.1002/adsc.200390027**.

38 Y. Wang, Z. Huang, G. Liu and Z. Huang, A New Paradigm in Pincer Iridium Chemistry: PCN Complexes for (De) Hydrogenation Catalysis and Beyond, *Acc. Chem. Res.*, 2022, **55**(15), 2148–2161, DOI: **10.1021/acs.accounts.2c00311**.

39 S. J. Roseblade and A. Pfaltz, Recent Advances in Iridium-Catalysed Asymmetric Hydrogenation of Unfunctionalised Olefins, *C. R. Chim.*, 2007, **10**(3), 178–187, DOI: **10.1016/j.crci.2006.12.001**.

40 (*a*) CCDC 2478806: Experimental Crystal Structure Determination, 2025, DOI: **10.5517/ccdc.csd.cc2p6dht**; (*b*) CCDC 2478807: Experimental Crystal Structure Determination, 2025, DOI: **10.5517/ccdc.csd.cc2p6djv**.